

Nonlinear ion acoustic waves in multicomponent plasmas with nonthermal electrons-positron and bipolar ions

Mai-Mai Lin(林麦麦), Chen-Guang Song(宋晨光), Fu-Yan Chen(陈富艳), and Ming-Yue Wang(王明月)

Citation: Chin. Phys. B, 2024, 33 (**12**): 125202. DOI: 10.1088/1674-1056/ad854f
Journal homepage: http://cpb.iphy.ac.cn; http://iopscience.iop.org/cpb

What follows is a list of articles you may be interested in

Ion acoustic solitary waves in an adiabatic dusty plasma: Roles of superthermal electrons, ion loss and ionization

Qianghua Rao(饶强华), Hui Chen(陈辉), Sanqiu Liu(刘三秋), and Xiaochang Chen(陈小昌)
Chin. Phys. B, 2024, 33 (**8**): 085201. DOI: 10.1088/1674-1056/ad47e4

Differences between two methods to derive a nonlinear Schrödinger equation and their application scopes

Yu-Xi Chen(陈羽西), Heng Zhang(张恒), and Wen-Shan Duan(段文山)
Chin. Phys. B, 2024, 33 (**2**): 025203. DOI: 10.1088/1674-1056/ad082b

The (1+1)-dimensional nonlinear ion acoustic waves in multicomponent plasma containing kappa electrons

Mai-Mai Lin(林麦麦), Lei Jiang(蒋蕾), and Ming-Yue Wang(王明月)
Chin. Phys. B, 2023, 32 (**12**): 125201. DOI: 10.1088/1674-1056/ace8f9

Effect of sharp vacuum-plasma boundary on the electron injection and acceleration in a few-cycle laser driven wakefield

Guo-Bo Zhang(张国博), Song Liu(刘松), De-Bin Zou(邹德滨), Ye Cui(崔野), Jian-Peng Liu(刘建鹏), Xiao-Hu Yang(杨晓虎), Yan-Yun Ma(马燕云), and Fu-Qiu Shao(邵福球)
Chin. Phys. B, 2023, 32 (**9**): 095202. DOI: 10.1088/1674-1056/acdc0c

Features of transport induced by ion-driven trapped-electron modes in tokamak plasmas

Hui Li(李慧), Ji-Quan Li(李继全), Feng Wang(王丰), Qi-Bin Luan(栾其斌),Hong-En Sun(孙宏恩), and Zheng-Xiong Wang(王正汹)
Chin. Phys. B, 2023, 32 (**7**): 075206. DOI: 10.1088/1674-1056/acae7e

---

Nonlinear ion acoustic waves in multicomponent plasmas with nonthermal electrons–positron and bipolar ions

Mai-Mai Lin(林麦麦)[†], Chen-Guang Song(宋晨光), Fu-Yan Chen(陈富艳), and Ming-Yue Wang(王明月)

College of Physics and Electronic Engineering, Northwest Normal University, Lanzhou 730070, *China*

(Received 22 July 2024; revised manuscript received 4 October 2024; accepted manuscript online 10 October 2024)

This paper studied the propagating characteristics of (2+1)-dimensional nonlinear ion acoustic waves in a multicomponent plasma with nonthermal electrons, positrons, and bipolar ions. The dispersion relations are initially explored by using the small amplitude wave's dispersion relation. Then, the Sagdeev potential method is employed to study large amplitude ion acoustic waves. The analysis involves examining the system's phase diagram, Sagdeev potential function, and solitary wave solutions through numerical solution of an analytical process in order to investigate the propagation properties of nonlinear ion acoustic waves under various parameters. It is found that the propagation of nonlinear ion acoustic waves is subject to the influence of various physical parameters, including the ratio of number densities between the unperturbed positrons, electrons to positive ions, nonthermal parameters, the mass ratio of positive ions to negative ions, and the charge number ratio of negative ions to positive ions, the ratio of the electrons' temperature to positrons' temperature. In addition, the multicomponent plasma system has a compressive solitary waves with amplitude greater than zero or a rarefactive solitary waves with amplitude less than zero, in the meantime, compressive and rarefactive ion acoustic wave characteristics depend on the charge number ratio of negative ions to positive ions.

Keywords: nonlinear ion acoustic waves, nonthermal electrons, bipolar ions, Sagdeev potential method

PACS: 52.35.Mw, 05.45.Yv, 47.20.Ky **DOI:** 10.1088/1674-1056/ad854f

1. Introduction

In recent decades, the structure of various waves has been extensively discussed, especially the theoretical and experimental studies of the nonlinear dynamics of ion acoustic waves have been intensively investigated.[1–3] The propagation of nonlinear ion acoustic waves in cold plasma was first investigated by Washimi *et al.*[4] On the other hand, ion acoustic waves in plasma were first observed experimentally by Ikezi *et al.*[5] Since then, ion acoustic waves have been studied extensively.[6–10]

Multiple studies highlight the importance of nonequilibrium, rapidly distributed nonthermal particles found in both laboratory and space models. It is shown that different distribution conditions have an important influence on the nonlinear process of ion acoustic waves.[11–17] For example, Lin *et al.* studied large amplitude nonlinear ion acoustic waves in a multicomponent plasma containing Kappa electron distribution. It is found that the number of Kappa electrons have important effect on the propagation of nonlinear ion acoustic waves.[18] Sabry *et al.* investigated the effect of nonthermal distribution of electrons on nonlinear ion acoustic waves. The results showed that the nonthermal parameters play a key role in the formation of ion acoustic waves.[19] On the other hand, the study of ionic pairs (IP) and electrons–positrons–ions (EPI) in plasmas performs a useful investigation for the propagating wave characteristics in many astrophysical and laboratory wave applications.[20–22] Electron–positrons are found in Van Allen belts and near the polar caps of rapidly rotating neutron stars, the early universe, the active galactic nuclei, the pulsar magnetosphere, *etc.*[23–28] Jannat *et al.* investigated the nonlinear propagation of ion acoustic shock waves containing nonextensive distributions of electrons and positrons. It is found that different plasma parameters create ion acoustic shock waves with positive and negative potentials.[29] Singh *et al.* studied the evolution and characterization of ion acoustic solitary waves (IASW) in a multicomponent plasma consisting of thermally inertial ions, superthermal electrons, and positrons. It is demonstrated that the positron density and the superthermal index of electrons and positrons play a key role in the formation of IASW.[30]

The large amplitude ion acoustic waves in a four-component plasma consisting of nonthermal electron–positron distribution and bipolar ions have rarely been studied. There are many effective methods for studying plasma wave phenomena. Among them, the Sagdeev potential method has been widely used as a tool for investigating arbitrary amplitude wave processes.[31–35] In this paper, the small amplitude wave's dispersion relation and the Sagdeev potential method have been used to investigate the impact of physical parameters on the propagating characteristics of nonlinear ion acoustic waves in this multicomponent plasma. Firstly, a theoretical model of (2+1)-dimensional nonlinear ion acoustic waves in a multicomponent plasma system consisting of positive ions, negative ions, and nonthermal distributed electrons and positrons is presented. Secondly, the critical Mach number

[†]Corresponding author. E-mail: linmaimai1514@126.com

© 2024 Chinese Physical Society and IOP Publishing Ltd

of the system is obtained, and the dispersion relation of the nonlinear ion acoustic waves is analyzed using the linearized method. The specific expression of the two-dimensional (2D) autonomous system, the Sagdeev potential equation, and the Sagdeev potential function are derived using the Sagdeev potential method. Finally, the phase diagram of the 2D autonomous system, the Sagdeev potential function, and the nonlinear ion acoustic solitary waves are discussed in detail with the help of numerical solution of an analytical process.

2. Theoretical model

In order to study the nonlinear ion acoustic waves in multicomponent plasma, it is assumed that there is a multicomponent plasma, consisting of positive ions, negative ions, nonthermal distributed electrons and positrons. Additionally, the plasma fluid is considered to evolve in two spatial dimensions, x and y, and one temporal dimension t, resulting in the dimensionless evolution equation for the (2+1)-dimensional nonlinear ion acoustic waves, the schematic diagram is shown in Fig. 1.



Fig. 1. The physical setup of the plasma system.

As is well known, the continuity equations for negative ions and positive ions are expressed as follows:[36]

$$\frac{\partial N_{\mathrm{n,p}}}{\partial t}+\frac{\partial}{\partial x}\left(N_{\mathrm{n,p}}U_{\mathrm{n,p}}\right)+\frac{\partial}{\partial y}\left(N_{\mathrm{n,p}}V_{\mathrm{n,p}}\right)=0, \tag{1}$$

the momentum equations in x and y directions for negative and positive ions are:

$$\frac{\partial U_{\mathrm{n}}}{\partial t}+U_{\mathrm{n}}\frac{\partial U_{\mathrm{n}}}{\partial x}+V_{\mathrm{n}}\frac{\partial U_{\mathrm{n}}}{\partial y}-Z_{\mp}Q\frac{\partial \phi}{\partial x}=0, \tag{2}$$

$$\frac{\partial V_{\mathrm{n}}}{\partial t}+U_{\mathrm{n}}\frac{\partial V_{\mathrm{n}}}{\partial x}+V_{\mathrm{n}}\frac{\partial V_{\mathrm{n}}}{\partial y}-Z_{\mp}Q\frac{\partial \phi}{\partial y}=0, \tag{3}$$

$$\frac{\partial U_{\mathrm{p}}}{\partial t}+U_{\mathrm{p}}\frac{\partial U_{\mathrm{p}}}{\partial x}+V_{\mathrm{p}}\frac{\partial U_{\mathrm{p}}}{\partial y}+\frac{\partial \phi}{\partial x}=0, \tag{4}$$

$$\frac{\partial V_{\mathrm{p}}}{\partial t}+U_{\mathrm{p}}\frac{\partial V_{\mathrm{p}}}{\partial x}+V_{\mathrm{p}}\frac{\partial V_{\mathrm{p}}}{\partial y}+\frac{\partial \phi}{\partial y}=0. \tag{5}$$

The Poisson equation is

$$\frac{\partial^2\phi}{\partial x^2}+\frac{\partial^2\phi}{\partial y^2}+N_{\mathrm{p}}-\alpha_{\mathrm{n}}N_{\mathrm{n}}=n_{\mathrm{e}}-n_{\mathrm{po}}, \tag{6}$$

where $N_{\mathrm{n,p}}$ are the dimensionless number of negative and positive ions, which normalized by its equilibrium value N_{n0} and N_{p0} respectively. $U_{\mathrm{n,p}}$ and $V_{\mathrm{n,p}}$ are the fluid velocities of negative and positive ions in x and y directions, which normalized by the negative and positive ion fluid velocities $C_{\mathrm{s}}=\left(K_{\mathrm{B}}T_{\mathrm{e}}/m_{\mathrm{p}}\right)^{1/2}$, where K_{B} is the Boltzmann constant, T_{e} is the electronic temperature, m_{p} the mass of the positive ion, respectively. The time variables t are normalized by the inverse of plasma frequency

$$\omega_{\mathrm{pi}}^{-1}=\left(m_{\mathrm{p}}/4\pi e^2Z_{+}^2N_{\mathrm{p0}}\right)^{1/2},$$

where Z_{+} is charge numbers of positive ions. $\omega_{\mathrm{pi}}^{-1}$ is the typical characteristic time of ion oscillations, using $\omega_{\mathrm{pi}}^{-1}$ as the characteristic time can reflect the response time of the plasma to perturbations. The space variables x and y are normalized by the Debye length

$$\lambda_{\mathrm{D}}=K_{\mathrm{B}}T_{\mathrm{e}}/4\pi e^2Z_{\mp}^2m_{\mathrm{p0}},$$

where $Z_{\mp}=Z_{-}/Z_{+}$ is charge numbers of negative to positive ions. λ_{D} is the characteristic length of charge shielding effect in plasma, using λ_{D} as the characteristic length can reflect the fluctuation on different spatial scales. The electrostatic potential ϕ is normalized by $K_{\mathrm{B}}T_{\mathrm{e}}/eZ_{+}$. $Q=m_{\mathrm{p}}/m_{\mathrm{n}}$ is the ratio of the mass, where m_{p} and m_{n} are the heavy and light ion fluid mass, respectively. $\alpha_{\mathrm{n}}=Z_{-}N_{\mathrm{n0}}/Z_{+}N_{\mathrm{p0}}$ represents the unperturbed number density ratio of negative ion to positive ion, detailed as follows:[36–38]

$$N_{\mathrm{n,p}}=\frac{N'_{\mathrm{n,p}}}{N_{\mathrm{n0,p0}}},\quad U_{\mathrm{n,p}}=\frac{U'_{\mathrm{n,p}}}{C_{\mathrm{s}}},\quad V_{\mathrm{n,p}}=\frac{V'_{\mathrm{n,p}}}{C_{\mathrm{s}}},\quad t=\frac{t'}{\omega_{\mathrm{pi}}^{-1}},$$

$$x=\frac{x'}{\lambda_{\mathrm{D}}},\quad y=\frac{y'}{\lambda_{\mathrm{D}}},\quad \phi=\frac{\phi'}{K_{\mathrm{B}}T_{\mathrm{e}}/eZ_{+}}.$$

The observations of space plasma showed that there are a lot of nonthermal distributed electrons exist in the space plasma. The nonthermal distributed expressions of electrons and positrons in Poisson equation are expressed as follows:[39]

$$n_{\mathrm{e}}=\alpha_{\mathrm{e}}\left(1-\beta\phi+\beta\phi^2\right)\mathrm{e}^{\phi}, \tag{7}$$

$$n_{\mathrm{po}}=\alpha_{\mathrm{p}}\left(1+\sigma\beta\phi+\sigma^2\beta\phi^2\right)\mathrm{e}^{-\sigma\phi}, \tag{8}$$

where $\alpha_{\mathrm{e}}=N_{\mathrm{e0}}/Z_{+}N_{\mathrm{p0}}$, $\alpha_{\mathrm{p}}=N_{\mathrm{p}o}/Z_{+}N_{\mathrm{p0}}$, where N_{e0} is the unperturbed electron density. The parameter $\sigma=T_{\mathrm{e}}/T_{\mathrm{po}}$ is the ratio of the electrons' temperature to positrons' temperature. $\beta=4\delta/1+3\delta$, where δ is the population of nonthermal electrons and positrons. The equilibrium condition is given by $\alpha_{\mathrm{n}}+\alpha_{\mathrm{e}}=1+\alpha_{\mathrm{p}}$.

3. Small amplitude nonlinear wave's dispersion relation

In order to derive the nonlinear dispersion relation of the nonlinear ion acoustic waves, equations (1)–(6) have been linearized as follows:

$$N_{\mathrm{n,p}}=1+\varepsilon N_{\mathrm{n,p}}^{(1)}\cdot\mathrm{e}^{\mathrm{i}\left(k_xx+k_yy-\omega t\right)},$$

$$U_{\mathrm{n,p}}=\varepsilon\cdot U_{\mathrm{n,p}}^{(1)}\cdot\mathrm{e}^{\mathrm{i}\left(k_xx+k_yy-\omega t\right)},$$

$$V_{\mathrm{n,p}}=\varepsilon\cdot V_{\mathrm{n,p}}^{(1)}\cdot\mathrm{e}^{\mathrm{i}\left(k_xx+k_yy-\omega t\right)},$$

$$\phi=\varepsilon\cdot\phi^{(1)}\cdot\mathrm{e}^{\mathrm{i}\left(k_xx+k_yy-\omega t\right)},$$

where k_x and k_y are the wave numbers in x and y directions and ω is the wave frequency.

In both the space and laboratory environments' plasma, there exist different kinds of multicomponent plasma, such as the $\left(H^+, O_2^-\right)$ and (H^+, H^-) multicomponent plasmas in the D_- and F^- regions of the Earth's ionosphere, the (Ar^+, F^-) multicomponent plasmas in the laboratory plasma. These kinds of plasmas, exhibit varying mass ratios Q due to their different compositional components. The mass ratio has an effect on the propagating characteristics of nonlinear ion acoustic waves. Notably, the mass ratios for $\left(H^+, O_2^-\right)$, (H^+, H^-), and (Ar^+, F^-) plasmas are 0.03, 1, and 2.1, respectively.[36,39] The dispersion relation of nonlinear ion acoustic waves is determined as

$$\omega^2 = \frac{\left(2-\alpha_e+\alpha_p\right)\cdot Q\cdot Z_{\mp}\cdot\left(k_x^2+k_y^2\right)}{\alpha_e-\alpha_e\cdot\frac{4\delta}{1+4\delta}+\alpha_p\cdot\sigma+\left(k_x^2+k_y^2\right)}. \tag{9}$$

The propagation of nonlinear ion acoustic waves in a four-component plasma which values containing of the positive ions, negative ions, nonthermal distributed electrons and positrons have been studied in detail, depending on the following parameters: α_p, α_e, δ, Q, $Z_{\mp}$, and σ, respectively. Figure 1 depicts the variations of dispersion relation under different parameter values when $k_y = 0$. The results show that ω^2 increases with the increases of parameters α_p, δ, Q, $Z_{\mp}$, k_x. An increase in positron number density weakens the plasma screening effect, allowing the ion acoustic waves to propagate with higher frequencies. Similarly, a higher nonthermal parameter δ indicates a larger proportion of energetic particles in the plasma, which accelerates the wave propagation and increases the frequency.

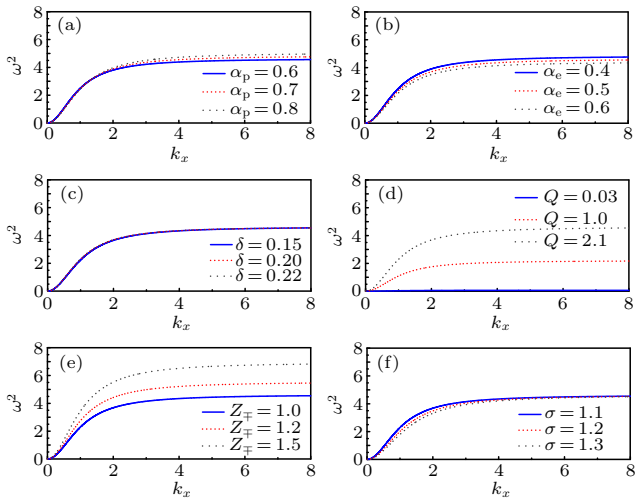


Fig. 2. The variations of dispersion relation with different parameters: (a) $\alpha_p = 0.6, 0.7, 0.8$, the fixed parameters are $\sigma = 1.1$, $\alpha_e = 0.5$, $\delta = 0.2$, $Q = 2.1$, $Z_{\mp} = 1$, and $k_y = 0$; (b) $\alpha_e = 0.4, 0.5, 0.6$, the fixed parameters are $\sigma = 1.1$, $\alpha_p = 0.7$, $\delta = 0.2$, $Q = 2.1$, $Z_{\mp} = 1$, and $k_y = 0$; (c) $\delta = 0.15$, 0.2, 0.22, the fixed parameters are $\sigma = 1.1$, $\alpha_p = 0.7$, $\alpha_e = 0.5$, $Q = 2.1$, $Z_{\mp} = 1$, and $k_y = 0$; (d) $Q = 0.03$, 1.0, 2.1, the fixed parameters are $\sigma = 1.1$, $\alpha_p = 0.7$, $\alpha_e = 0.5$, $\delta = 0.2$, $Z_{\mp} = 1$, and $k_y = 0$; (e) $Z_{\mp} = 1.0$, 1.2, 1.3, the fixed parameters are $\sigma = 1.1$, $\alpha_p = 0.7$, $\alpha_e = 0.5$, $\delta = 0.2$, $Q = 2.1$, and $k_y = 0$; (f) $\sigma = 1.1$, 1.2, 1.3, the fixed parameters are $\alpha_p = 0.7$, $\alpha_e = 0.5$, $\delta = 0.2$, $Q = 2.1$, $Z_{\mp} = 1$, and $k_y = 0$.

Moreover, as the mass ratio Q increases, despite the added inertial effect of heavier positive ions, the stronger electric field restoring force enhances wave propagation, resulting in higher frequencies. The charge number ratio $Z_{\mp}$ also plays a role: an increase in this ratio strengthens the restoring force between positive and negative ions, further raising the propagation frequency.

On the other hand, it can be seen from Figs. 2(b) and 2(f) that ω^2 decreases gradually when the parameters α_e, σ increase gradually. When the electron density radio α_e and the electron temperature radio σ increase, higher electron density enhances the screening effect, which diminishes the restoring force of the electric field, lowering the frequency. Similarly, an increase in electron temperature increases the speed of thermal motion, strengthening the screening effect and reducing the wave frequency.

This indicates that the propagation frequency of the ion acoustic wave is higher when the unperturbed number density ratio of the positron to positive ions, nonthermal parameters, the mass ratio of positive ions to negative ions, and the charge number ratio of negative ions to positive ions increase. At the same time, there are some effects of other parameters on the propagation frequency of the nonlinear ion acoustic wave.

In addition, figure 2(f) shows that the nonlinear ion acoustic wave propagates at a very low frequency when $Q = 0.03$. It can be seen that the mass ratio Q of positive ions to negative ions plays an important role in the propagation frequency of nonlinear ion acoustic waves.

4. Propagating characters of large amplitude nonlinear waves

To obtain the propagating characters of the large amplitude nonlinear ion acoustic waves in the system, a new variable $\xi = l_x x + l_y y - Mt$ is introduced, where l_x and l_y represent the wave numbers in the x and y directions respectively, and M is the Mach number associated with the localized wave. Consequently, the system of negative ions can be transformed into ordinary differential equations in terms of the variable ξ

$$\begin{aligned}
&-M\cdot\frac{\mathrm{d}N_n}{\mathrm{d}\xi}+l_x\cdot\frac{\mathrm{d}\left(N_nU_n\right)}{\mathrm{d}\xi}+l_y\cdot\frac{\mathrm{d}\left(N_nU_n\right)}{\mathrm{d}\xi}=0,\\
&-M\cdot\frac{\mathrm{d}U_n}{\mathrm{d}\xi}+U_n\cdot l_x\cdot\frac{\mathrm{d}\left(U_n\right)}{\mathrm{d}\xi}+V_n\cdot l_y\cdot\frac{\mathrm{d}\left(U_n\right)}{\mathrm{d}\xi}\\
&-Z_{\mp}\cdot Q\cdot l_x\cdot\frac{\mathrm{d}\left(\phi\right)}{\mathrm{d}\xi}=0,\\
&-M\cdot\frac{\mathrm{d}V_n}{\mathrm{d}\xi}+U_n\cdot l_x\cdot\frac{\mathrm{d}\left(V_n\right)}{\mathrm{d}\xi}+V_n\cdot l_y\cdot\frac{\mathrm{d}\left(V_n\right)}{\mathrm{d}\xi}\\
&-Z_{\mp}\cdot Q\cdot l_x\cdot\frac{\mathrm{d}\left(\phi\right)}{\mathrm{d}\xi}=0.
\end{aligned}$$

Integrating the relationship given above and utilizing the following boundary conditions:[37] $\xi \to \pm\infty$, $N_{n,p} \to 1$, $U_{n,p} \to 0$,

$V_{n,p} \to 0$, and $\phi \to 0$, we obtain

$$N_n = \sqrt{\frac{M^2}{M^2+2Q\phi Z_{\mp}}}. \tag{10}$$

For positive ions,

$$-M\frac{dN_p}{d\xi} + l_x\frac{d\left(N_pU_p\right)}{d\xi} + l_y\frac{d\left(N_pU_p\right)}{d\xi} = 0,$$
$$-M\frac{dU_p}{d\xi} + U_pl_x\frac{d\left(U_p\right)}{d\xi} + V_pl_y\frac{d\left(U_p\right)}{d\xi} + l_x\frac{d\left(\phi\right)}{d\xi} = 0,$$
$$-M\frac{dV_p}{d\xi} + U_pl_x\frac{d\left(V_p\right)}{d\xi} + V_pl_y\frac{d\left(V_p\right)}{d\xi} + l_y\frac{d\left(\phi\right)}{d\xi} = 0.$$

Similarly, we can obtain

$$N_p = \sqrt{\frac{M^2}{M^2-2\phi}}. \tag{11}$$

For the Poisson equation,

$$\frac{d^2\phi}{d\xi^2} + N_p - \alpha_nN_n = \alpha_e\left(1-\beta\phi+\beta\phi^2\right)e^{\phi} - \alpha_p\left(1+\sigma\beta\phi+\sigma^2\beta\phi^2\right)e^{-\sigma\phi}. \tag{12}$$

Substituting Eqs. (10) and (11) into the Poisson equation (12) and expanding the resulting expression, we obtain

$$\frac{d^2\phi}{d\xi^2} = A_1\phi + A_2\phi^2, \tag{13}$$

where

$$A_1 = \left(-\frac{1}{M^2} - \frac{4\delta}{1+3\delta} + 1\right)\alpha_e - \frac{Q\cdot Z_{\mp}\cdot\alpha_n}{M^2} + \sigma\left(-\frac{4\delta}{1+3\delta}+1\right)\alpha_p,$$
$$A_2 = \frac{1}{2}\cdot\left(-\frac{3}{M^4} + \alpha_e + \frac{3Q^2\cdot Z_{\mp}^2\cdot\alpha_n}{M^4} + 1\right) - \sigma^2\alpha_p.$$

Transform Eq. (13) into a 2D autonomous system

$$\begin{cases} \dfrac{d\phi}{d\xi} = \Psi, \\ \dfrac{d\Psi}{d\xi} = A_1\phi + A_2\phi^2. \end{cases} \tag{14}$$

Now, multiplying Eq. (13) by $d\varphi/d\xi$, integrating the resulting expression once, we can obtain the Sagdeev potential equation

$$\frac{1}{2}\left(\frac{d\phi}{d\xi}\right)^2 + V(\phi) = 0, \tag{15}$$

where the Sagdeev potential $V(\phi)$ is defined as follows:

$$V(\phi) = -\frac{1}{2}A_1\phi^2 - \frac{1}{3}A_2\phi^3. \tag{16}$$

The advantage of employing the Sagdeev potential technique lies in our ability to detect the presence of solitary waves under certain conditions:[40]

(i) $V(\phi) = 0$ at $\phi = 0$ and $\phi = \phi_m$, where ϕ_m is the maximum value of ϕ;

(ii) $dV(\phi)/d\phi = 0$ at $\phi = 0$, so that the fixed point at the origin is unstable;

(iii) $d^2V/d\phi^2 < 0$ at $\phi = 0$.

It is important to highlight that $V(\phi) < 0$ for ϕ between 0 and ϕ_m, *i.e.*, when the condition $\phi < \phi_m < 0$ is satisfied, the system exhibits rarefactive solitary waves and if the condition $0 < \phi_m < \phi$ is meet, the compressive solitary waves emerge in the system. Since the Mach number M enters as a free parameter whose allowed range of values has to be determined. For the third condition (iii): $d^2V/d\phi^2 < 0$ at $\phi = 0$, we can obtain the critical value of Mach number M_{cr}:[40]

$$M_{cr} = \sqrt{\frac{1+3\delta+Q\cdot Z_{\mp}\cdot\alpha_n+3\cdot Q\cdot Z_{\mp}\cdot\alpha_n\cdot\delta+\sqrt{\left(-1-3\delta-Q\cdot Z_{\mp}\cdot\alpha_n-3Q\cdot Z_{\mp}\cdot\alpha_n\cdot\delta\right)^2}}{2\left(\alpha_e-\delta\cdot\alpha_e+\sigma\cdot\alpha_p-\delta\cdot\sigma\cdot\alpha_p\right)}}. \tag{17}$$

The variations of critical Mach number with different parameters is shown in Fig. 3, from which it can be seen that the critical Mach number depends on the parameters α_p, α_e, δ, Q, $Z_{\mp}$, and σ, the acceptable minimum Mach number decreases progressively with the increase of parameters α_p, α_e, and σ. This indicates that an increase in physical quantities, such as the ratio of number densities of positron, electrons to positive ions, the temperature ratio between electrons and

positrons leads to a decrease in the minimum Mach number required for the presence of ion acoustic waves. The critical Mach number is a key parameter that determines the existence and propagation of the solitary waves. Only when the Mach number exceeds a certain critical value, can a solitary wave form and propagate stably. Conversely, when the Mach number is below the critical value, a stable solitary wave cannot form. For instance, when the system parameters are $\sigma = 1.1$, $\alpha_e = 0.5$, $M = 3.0$, $\delta = 0.2$, $Z_{\mp} = 1$, and $Q = 2.1$, the minimum Mach numbers required to form stable solitary waves are 2.53, 2.35, and 2.20, respectively. However, as other parameters gradually increase, the range of the minimum Mach number accepted by ion acoustic waves gradually increases.

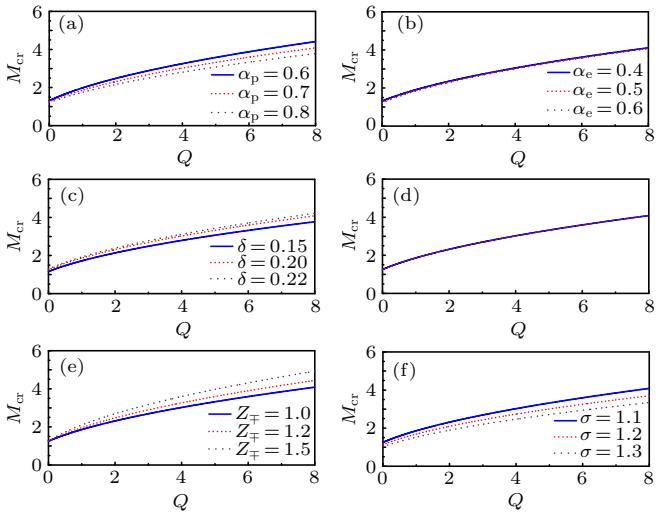


Fig. 3. The variations of critical Mach number with different parameters: (a) $\alpha_p = 0.6, 0.7, 0.8$, the fixed parameters are $\sigma = 1.1$, $\alpha_e = 0.5$, $\delta = 0.2$, and $Z_{\mp} = 1$; (b) $\alpha_e = 0.4, 0.5, 0.6$, the fixed parameters are $\sigma = 1.1$, $\alpha_p = 0.7$, $\delta = 0.2$, $Z_{\mp} = 1$; (c) $\delta = 0.15, 0.2, 0.22$, the fixed parameters are $\sigma = 1.1$, $\alpha_p = 0.7$, $\alpha_e = 0.5$, and $Z_{\mp} = 1$; (d) the fixed parameters are $\sigma = 1.1$, $\alpha_p = 0.7$, $\alpha_e = 0.5$, $\delta = 0.2$, $Z_{\mp} = 1$; (e) $Z_{\mp} = 1.0, 1.2, 1.5$, the fixed parameters are $\sigma = 1.1$, $\alpha_p = 0.7$, $\alpha_e = 0.5$, $\delta = 0.2$; (f) $\sigma = 1.1, 1.2, 1.3$, the fixed parameters are $\alpha_p = 0.7$, $\alpha_e = 0.5$, $\delta = 0.2$, and $Z_{\mp} = 1$.

5. Results and discussion

In order to study the different types of waves present in a multicomponent plasma with nonthermal electrons and bipolar ions, the influence of various parameters on the nonlinear dynamical system (14) have been analyzed.

Figures 4–9 depict the variations in the phase diagram of a complex plasma system under different parameter conditions. From the phase diagrams, it can be observed the existence of linear periodic wave orbits (LPOs) and nonlinear periodic wave orbits (NPOs) centered around the central point, as well as the homoclinic orbits (NHOs) that originate from a saddle point and return to the same saddle point. This implies the simultaneous presence of the linear periodic wave solutions, the nonlinear periodic wave solutions, and the solitary wave solutions in the system.[40]

Figure 4 illustrates the variations of the phase diagram for different parameter values. The other parameters are taken as $\sigma = 1.1$, $\alpha_e = 0.5$, $M = 3.0$, $\delta = 0.2$, $Z_{\mp} = 1$, and $Q = 2.1$, respectively. It can be seen that the range of existence for the phase diagram decreases rapidly when the values of parameter α_p increase from 0.6 to 0.8. This indicates that the presence of positron number density has an effect on the distribution of linear periodic wave orbitals, nonlinear periodic wave orbitals, and homoclinic orbits in the phase space. Specifically, as the system parameter α_p gradually increases, the existence range of various orbits in the phase diagram gradually narrows. This indicates that the range of existence for solitary wave solutions also decreases correspondingly, and the phase space position of the solitary wave solutions shifts. Furthermore, it can be observed from the figure that as the parameter α_p increases, the amplitude ϕ of the solitary wave corresponding to the homoclinic orbit gradually decreases. This is validated in the subsequent discussion on solitary waves.

Figure 5 illustrates the variations of the phase diagram for different values of α_e, the values of other parameters are $\sigma = 1.1$, $\alpha_p = 0.7$, $M = 3.0$, $\delta = 0.2$, $Z_{\mp} = 1$, and $Q = 2.1$, respectively. It can be seen that the existence range of the phase diagram tends to increase with the gradual increase of α_e. It is noteworthy that the existence range of various nonlinear waves is relatively larger when the value of α_e is 0.8. This phenomenon indicates that the presence of electron number density is favorable to expand the existence range of various nonlinear waves. Specifically, as the system parameter α_e gradually increases, the existence range of solitary wave solutions expands, and their position also changes. Additionally, as the parameter α_e increases, the amplitude ϕ of the solitary wave corresponding to the homoclinic orbit increases.

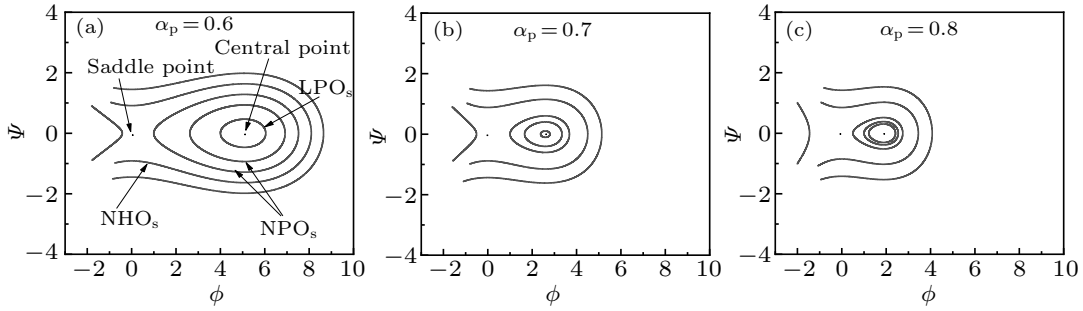


Fig. 4. The variations of system phase diagram with different values of α_p.

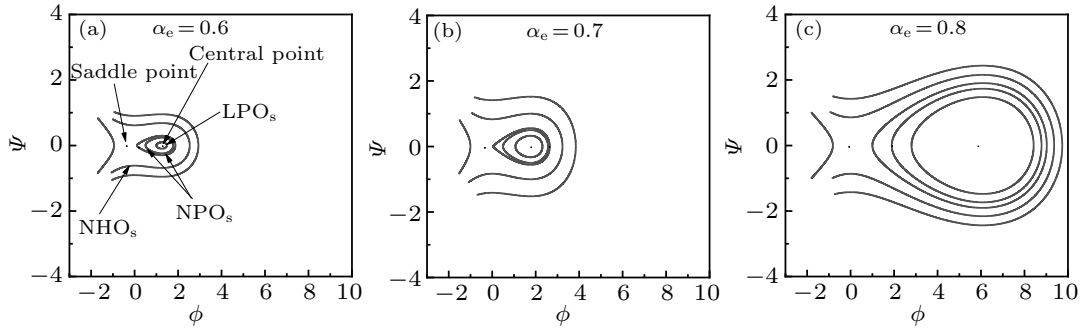


Fig. 5. The variations of system phase diagram with different values of α_e.

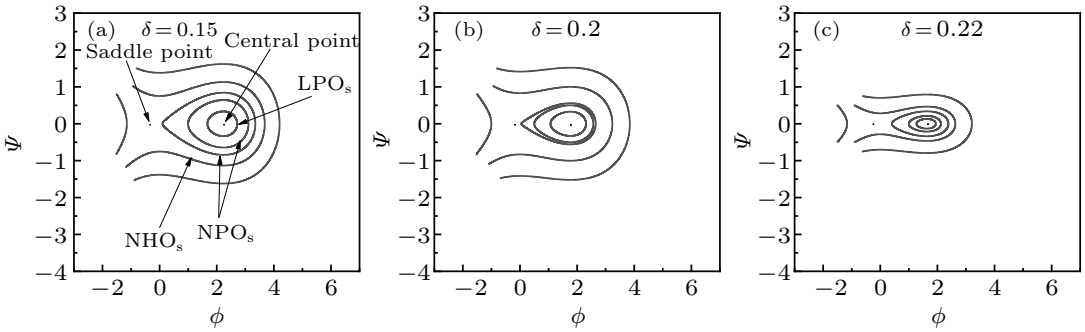


Fig. 6. The variations of system phase diagram with different values of δ.

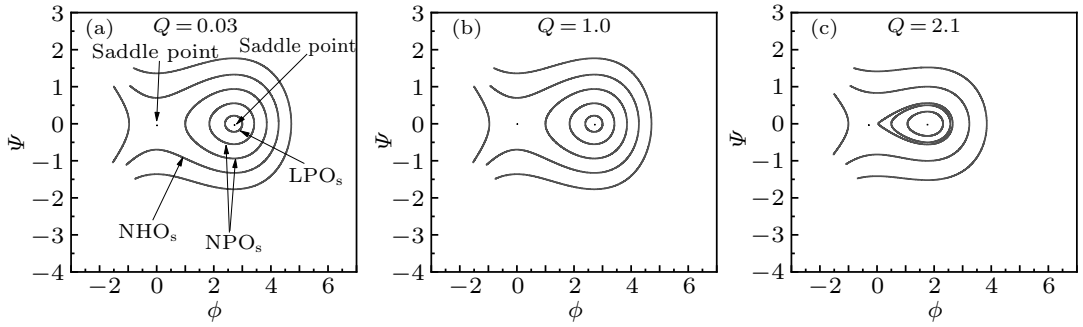


Fig. 7. The variations of system phase diagram with different values of Q.

Figure 6 shows the variations of the phase diagram for different values of δ. The other parameters are taken as $\sigma = 1.1$, $\alpha_p = 0.7$, $\alpha_e = 0.5$, $M = 3.0$, $Z_{\mp} = 1$, and $Q = 2.1$, respectively. From the figure, it can be seen that the range of the existence for the phase diagram decreases with the increase of δ, *i.e.*, the number of nonthermal electrons and positrons has some effects on the range of existence for the phase diagram of the system. This shows that: more numbers of nonthermal electrons and positrons reduce the range of existence for linear periodic wave solutions, nonlinear periodic wave solutions, and solitary wave solutions. In other words, when δ increases, the range and position of solitary wave solutions in phase space undergo significant compression. At the same time, the amplitude of the solitary wave decreases as δ increases. In the ionosphere, when nonthermal effects are significant, the propagation characteristics of ion acoustic waves are affected.

Figure 7 shows the variations of the phase diagram for different parameters of Q. The other parameters are taken as $\sigma = 1.1$, $\alpha_p = 0.7$, $\alpha_e = 0.5$, $M = 3.0$, $Z_{\mp} = 1$, and $Q = 2.1$, respectively. It can be found that the range of existence for the phase diagram decreases with the increase of Q. This indicates that: the larger mass ratio of negative ions to positive ions the smaller the range of existence of linear periodic wave solutions, nonlinear periodic wave solutions, and solitary wave solutions. The amplitude ϕ of the solitary wave on the homoclinic orbit decreases. This indicates that a larger mass ratio of positive to negative ions imposes a limiting effect on the propagation range of the waves in the ionosphere.

Figure 8 illustrates the variations of the phase diagram with different values of charge number ratios $Z_{\mp}$. It can be found that the range of the existence for the phase diagram gradually increases with increasing $Z_{\mp}$ as the negative to positive ion charge ratio increases from 1 to 1.2. However, it is noteworthy that the polarity of the phase diagram changes when $Z_{\mp} = 1.5$. This suggests that the change of the charge ratio for negative to positive ions affects the distribution of linear periodic wave orbitals, nonlinear periodic wave orbitals,

and homoclinic orbitals in the phase space, which in turn affects the range of existence of linear periodic wave solutions, nonlinear periodic wave solutions, and solitary wave solutions. Furthermore, it can be observed that as the charge number ratio of positive to negative ions gradually increases, the range and position of solitary wave solutions in phase space undergo significant expansion. At the same time, the amplitude of the solitary wave gradually increases with the increase of $Z_{\mp}$, and when $Z_{\mp} = 1.5$, the polarity of the phase diagram changes. This indicates that the charge number ratio of positive to negative ions in the ionosphere can alter the behavior of plasma fluctuations.

Figure 9 illustrates the variations of the phase diagram with different values of the electron to positron's temperature ratio σ. The other parameters are $\alpha_e = 0.5$, $\alpha_p = 0.7$, $M = 3.0$, $\delta = 0.2$, $Z_{\mp} = 1$ and $Q = 2.1$, respectively. It is found that the range of the existence for the phase diagram decreases gradually with the increase of the parameter σ. This indicates that the increase of the electron to positron temperature ratio significantly narrows the range of the existence for various nonlinear waves. In particular, the range of solitary wave solutions in phase space also decreases correspondingly, while the amplitude of the solitary wave decreases with the increase of σ. This temperature difference in the ionosphere affects the propagation characteristics of ion acoustic waves.

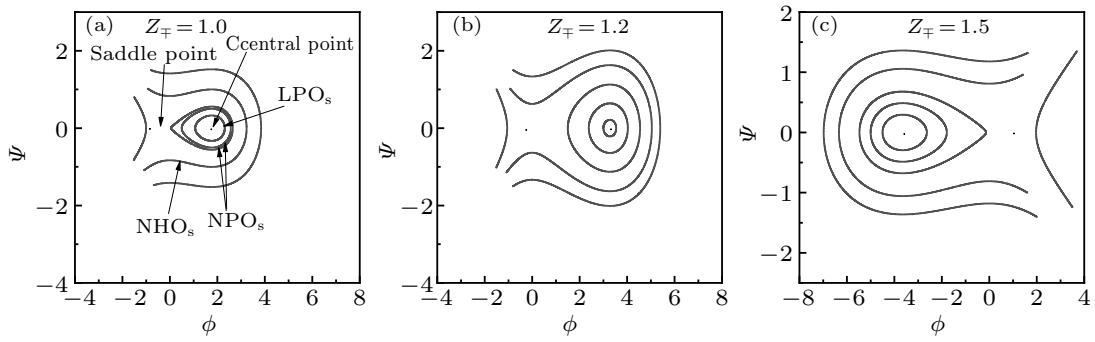


Fig. 8. The variations of system phase diagram with different values of $Z_{\mp}$.

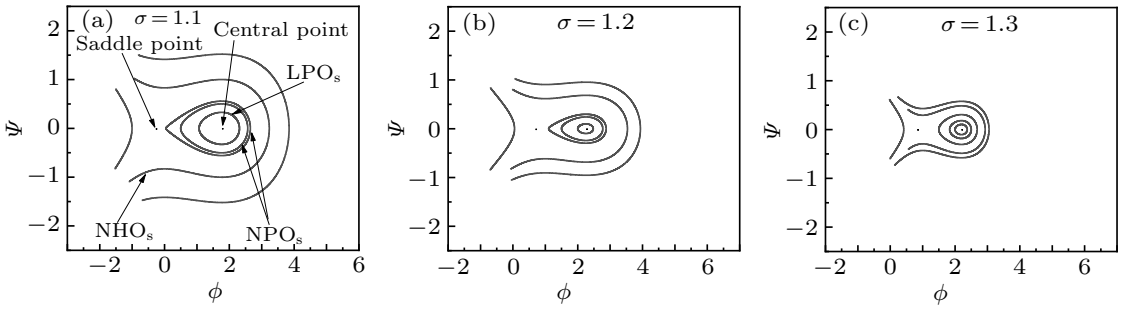


Fig. 9. The variations of system phase diagram with different values of σ.

From the phase diagram, it can be observed that the existence of homoclinic orbits is near the saddle point, indicating the presence of solitary wave solutions in the system. To demonstrate this, the Sagdeev potential $V(\phi)$ has been plotted to study the properties of solitary waves. Figure 10 illustrates the variations of the Sagdeev potential with different parameters.

Based on the previous discussion and the Sagdeev potential diagram, it is evident that under the given parameter values, the plasma system exhibits either compressive solitary waves with amplitudes greater than zero or rarefactive solitary waves with amplitudes less than zero. On the other hand, figure 10 indicates that as α_p, δ, Q, and σ increase gradually, the amplitude of ion acoustic waves decreases. Conversely, as α_e increases gradually, the amplitude of ion acoustic waves increases. It is worth noting that figure 10(e) shows that the solitary wave amplitude gradually increases with the increase of the system parameter $Z_{\mp}$ from 1 to 1.2, and when the value of 1.5 is taken, the solitary wave in the system is transformed from a compressive solitary wave to rarefactive solitary wave.

To clearly illustrate the waveform and the amplitude characteristics of solitary waves, the Sagdeev equation can be solved analytically and the ion acoustic solitary waves have been obtained:[41]

$$\phi = \phi_m \cdot \mathrm{sech}^2\left(\frac{\xi}{D}\right), \tag{18}$$

where the amplitude of solitary wave is

$$\phi_m = -\frac{3}{2}\frac{A_2}{A_3},$$

and the width of solitary wave is $D = \sqrt{4/A_2}$, respectively.

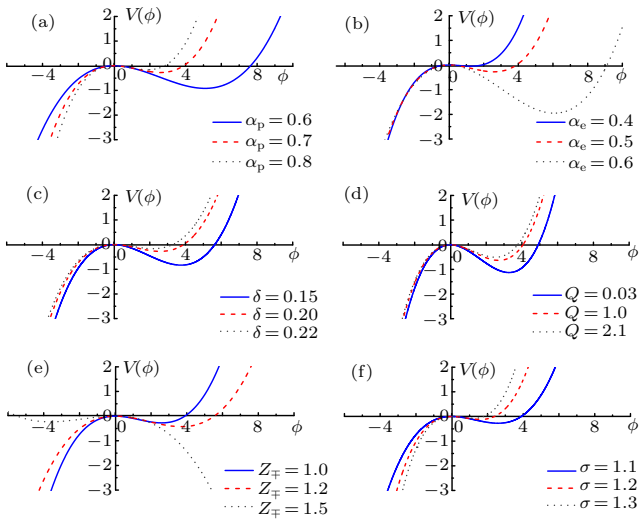


Fig. 10. The variations of Sagdeev potentia $V(\phi)$ with different parameters: (a) $\alpha_p = 0.6, 0.7, 0.8$, the fixed parameters are $\sigma = 1.1$, $\alpha_e = 0.5$, $\delta = 0.2$, $Q = 2.1$, $M = 3.0$, and $Z_{\mp} = 1$; (b) $\alpha_e = 0.4, 0.5, 0.6$, the fixed parameters are $\sigma = 1.1$, $\alpha_p = 0.7$, $\delta = 0.2$, $Q = 2.1$, $M = 3.0$, and $Z_{\mp} = 1$; (c) $\delta = 0.15, 0.2, 0.22$, the fixed parameters are $\sigma = 1.1$, $\alpha_p = 0.7$, $\alpha_e = 0.5$, $Q = 2.1$, $M = 3.0$, and $Z_{\mp} = 1$; (d) $Q = 0.03, 1.0, 2.1$, the fixed parameters are $\sigma = 1.1$, $\alpha_p = 0.7$, $\alpha_e = 0.5$, $\delta = 0.2$, $M = 3.0$, and $Z_{\mp} = 1$; (e) $Z_{\mp} = 1.0, 1.2, 1.5$, the fixed parameters are $\sigma = 1.1$, $\alpha_p = 0.7$, $\alpha_e = 0.5$, $\delta = 0.2$, $M = 3.0$, and $Q = 2.1$. (f) $\sigma = 1.1, 1.2, 1.3$, the fixed parameters are $\alpha_e = 0.5$, $\alpha_p = 0.7$, $M = 3.0$, $\delta = 0.2$, $Z_{\mp} = 1$, and $Q = 2.1$.

Figure 11 presents the specific evolution patterns of waveforms. Under the given parameter values, the plasma system exhibits either compressive solitary waves with amplitudes greater than zero or rarefactive solitary waves with amplitudes less than zero. Figures 11(a), 11(c), 11(d), and 11(f) show that the amplitude of the solitary wave gradually decreases while the width gradually increases as the system parameters increase. Figure 11(b) shows that the amplitude of the solitary wave gradually increases while the width gradually decreases as the system parameter increases. In addition, figure 11(e) shows that the amplitude of the solitary wave is gradually increasing when the system parameter increases from 1 to 1.2, and the solitary wave changes from a compressive solitary wave to a rarefactive solitary wave when $Z_{\mp}$ is set to 2.1. This conclusion agrees with the analytical results of the Sagdeev function in Fig. 10.

Considering the specific expressions of various parameters in the theoretical model, thus, the increase in physical quantities such as the positron to positive ion number density ratio, the mass ratio of positive to negative ions, the electron to positron temperature ratio, and the number of nonthermal electrons to positrons leads to a decrease in the amplitude of the solitary wave, an increase in its width, and a smoother, more extended solitary waves. Conversely, the increase in the electron to positive ion number density ratio results in an increased amplitude and decreased width of the solitary wave, making it sharper. Additionally, when the charge number ratio of negative to positive ions $Z_{\mp} = 1.5$, the direction and nature of the solitary wave change, transitioning from a compressive type to a rarefactive type. This is related to charge asymmetry.

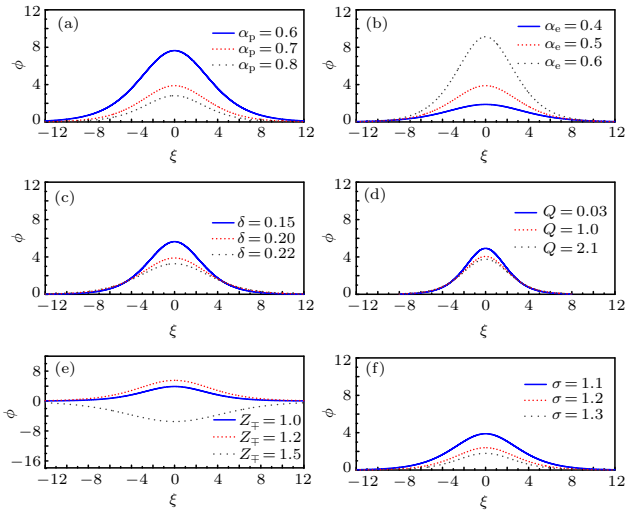


Fig. 11. The waveform variations of the solitary waves ϕ with different parameters: (a) $\alpha_p = 0.6, 0.7, 0.8$, the fixed parameters are $\sigma = 1.1$, $\alpha_e = 0.5$, $\delta = 0.2$, $Q = 2.1$, $M = 3.0$, and $Z_{\mp} = 1$; (b) $\alpha_e = 0.4, 0.5, 0.6$, the fixed parameters are $\sigma = 1.1$, $\alpha_p = 0.7$, $\delta = 0.2$, $Q = 2.1$, $M = 3.0$, and $Z_{\mp} = 1$; (c) $\delta = 0.15, 0.2, 0.22$, the fixed parameters are $\sigma = 1.1$, $\alpha_p = 0.7$, $\alpha_e = 0.5$, $Q = 2.1$, $M = 3.0$, and $Z_{\mp} = 1$; (d) $Q = 0.03, 1.0, 2.1$, the fixed parameters are $\sigma = 1.1$, $\alpha_p = 0.7$, $\alpha_e = 0.5$, $\delta = 0.2$, $M = 3.0$, and $Z_{\mp} = 1$; (e) $Z_{\mp} = 1.0, 1.2, 1.5$, the fixed parameters are $\sigma = 1.1$, $\alpha_p = 0.7$, $\alpha_e = 0.5$, $\delta = 0.2$, $M = 3.0$, and $Q = 2.1$. (f) $\sigma = 1.1, 1.2, 1.3$, the fixed parameters are $\alpha_e = 0.5$, $\alpha_p = 0.7$, $M = 3.0$, $\delta = 0.2$, $Z_{\mp} = 1$, and $Q = 2.1$.

6. Conclusion

This paper investigates the progress of (2+1)-dimensional nonlinear ion acoustic waves in multicomponent plasmas. Initially, the dispersion relations were obtained using a small amplitude wave's dispersion relation, and then the Sagdeev potential method was employed to derive the analytical expression of the Sagdeev potential. The propagation characteristics of nonlinear ion acoustic solitary waves under different system parameter values were analyzed based on the system phase diagrams, the Sagdeev potential functions, and the solitary waves. The study reveals that the propagation of nonlinear ion acoustic solitary waves is influenced by physical parameters such as the ratio of number densities between the unperturbed positrons, electrons to positive ions α_p, α_e, nonthermal parameters δ, the mass ratio of positive ions to negative ions Q, and the charge numbers ratio of negative ions to positive ions $Z_{\mp}$, the ratio of the electrons' temperature to positrons' temperature σ. Finally, the results of this study play an important role in understanding nonlinear phenomena in ionospheric and laboratory environments.

References

[1] Sarma R, Misra A P and Adhikary N C 2018 *Chin. Phys. B* **27** 105207
[2] Erheest F, Hellberg M A and Hereman W A 2012 *Phys. Rev. E* **86** 036402
[3] Singh S V and Lakhina G S 2015 *Commun. Nonlinear. Sci. Numer. Simul.* **23** 274
[4] Washimi H and Taniuti T 1966 *Phys. Rev. Lett.* **17** 966
[5] Ikezi H, Tailor R J and Baker D R 1970 *Phys. Rev. Lett.* **25** 11
[6] Lakhina G S, Singh S V, Kakad A P, Verheest F and Bharuthram R 2008 *Nonlinear. Process. Geophys.* **15** 903
[7] Saini N S and Shalini 2014 *Phys. Plasmas* **21** 102901

[8] Khan M, Irshad M, Khalid M and Rahman A 2021 *Z. Naturforsch. A* **77** 125
[9] Bukhari S, Shahid M and Rahman N A 2024 *Plasma. Sci. Technol.* **26** 015001
[10] Kusum C, Jharna T, Prasanta C and Saha A 2024 *Astrophysics. Space Sci.* **369** 44
[11] Selim M M 2016 *Eur. Phys. J. Plus* **131** 93
[12] Banerjee G and Maitra S 2016 *Phys. Plasmas* **23** 123701
[13] Paul A and Bandyopadhyay A 2018 *Indian J. Phys.* **92** 1187
[14] Farooq M, Mushtaq A and Qasim J 2018 *Contrib. Plasma Phys.* **59** 122
[15] El-Taibany W F, El-Siragy N M, Behery E E, El-Bendary A A and Taha R M 2019 *Chin. J. Phys.* **58** 151
[16] Madhukalya B, Kalita J, Das R, Hosseini K, Baleanu D and Osman M S 2024 *Opt. Quantum Electron.* **56** 898
[17] Alyousef H A, Naeem S N, Irshad M, Rahman A U, Ismaeel S M E and El-Tantawy S A 2024 *Phys. Fluids* **36** 035151
[18] Lin M M, Jiang L and Wang M Y 2023 *Chin. Phys. B* **32** 125201
[19] Sabry R, Moslem W M and Shukla P K 2009 *Phys. Plasmas* **16** 032302
[20] Erheest F, Hellberg M A and Hereman W A 2012 *Phys. Rev. E* **86** 036402
[21] Singh S V and Lakhina G S 2015 *Commun. Nonlinear. Sci. Numer. Simul.* **23** 274
[22] Guo S, Mei L and Zhang Z 2015 *Phys. Plasmas* **22** 052306
[23] Lightman A P 1982 *Astrophys. J.* **253** 842
[24] Abdelwahed H G, El-Shewy E K and Mahmoud A A 2017 *Chin. Phys. Lett.* **34** 035202
[25] Alam M S, Hafez M G, Talukder M R and Ali M H 2017 *Chin. Phys. B* **26** 095203
[26] Dev A N 2017 *Chin. Phys. B* **26** 025203
[27] Jian M J, Rong Y J and Ying L C 2012 *Acta Phys. Sin.* **61** 020206 (in Chinese)
[28] Surko C M, Leventhal M and Passner A 1989 *Phys. Rev. Lett.* **62** 901
[29] Jannat N, Ferdusi M and Mamun A A 2015 *Commun. Theor. Phys.* **64** 479
[30] Singh K, Kakad A, Kakad B and Saini N S 2020 *Eur. Phys. J. Plus* **136** 14
[31] Demiray H and Abdikian A 2019 *Chaos, Solitons and Fractals* **121** 50
[32] El-Hanbaly A M, El-Shewy E K, Sallah M and Darweesh H F 2016 *Commun. Theor. Phys.* **65** 606
[33] Mamun A A and Shukla P K 2009 *Europhys. Lett.* **87** 55001
[34] Hatami M M and Niknam A R 2021 *Physica A* **564** 125533
[35] Sebastian S, Sreekala G, Michael M, Abraham N P, Renuka G and Venugopal C 2015 *Phys. Scr.* **90** 035601
[36] Abdelwahed H G, Sabry R and El-Rahman A A 2021 *Chin. J. Phys.* **72** 670
[37] Bains A S, Saini N S and Gill T S 2013 *Can. J. Phys.* **91** 582
[38] Elwakil S A, El-Shewy E K and Abdelwahed H G 2010 *Phys. Plasmas* **17** 052301
[39] Khaled M A H, Shukri M A and Hager Y A A 2022 *Chin. Phys. B* **31** 010505
[40] Saha A and Tamang J 2018 *Adv. Space Res.* **63** 1596
[41] Saha A, Chatterjee P and Pal N 2015 *J. Plasma. Phys.* **81** 5